

Insights into the effect of susceptor rotational speed in CVD reactor on the quality of 4H-SiC epitaxial layer on homogeneous substrates

Tang, Zhuorui ; Gu, Lin ; Jin, Lei ; Dai, Kefeng ; Mao, Chaobin ; Wu, Sanzhong ; Zhang, Rongwei ; Yang, Jinsong; Zhang, Guoqi; More Authors

DOI

[10.1016/j.mtcomm.2024.108037](https://doi.org/10.1016/j.mtcomm.2024.108037)

Publication date

2024

Document Version

Final published version

Published in

Materials Today Communications

Citation (APA)

Tang, Z., Gu, L., Jin, L., Dai, K., Mao, C., Wu, S., Zhang, R., Yang, J., Zhang, G., & More Authors (2024). Insights into the effect of susceptor rotational speed in CVD reactor on the quality of 4H-SiC epitaxial layer on homogeneous substrates. *Materials Today Communications*, 38, Article 108037. <https://doi.org/10.1016/j.mtcomm.2024.108037>

Important note

To cite this publication, please use the final published version (if applicable). Please check the document version above.

Copyright

Other than for strictly personal use, it is not permitted to download, forward or distribute the text or part of it, without the consent of the author(s) and/or copyright holder(s), unless the work is under an open content license such as Creative Commons.

Takedown policy

Please contact us and provide details if you believe this document breaches copyrights. We will remove access to the work immediately and investigate your claim.

Green Open Access added to TU Delft Institutional Repository

'You share, we take care!' - Taverne project

<https://www.openaccess.nl/en/you-share-we-take-care>

Otherwise as indicated in the copyright section: the publisher is the copyright holder of this work and the author uses the Dutch legislation to make this work public.



Insights into the effect of susceptor rotational speed in CVD reactor on the quality of 4H-SiC epitaxial layer on homogeneous substrates

Zhuorui Tang^{a,b}, Lin Gu^{a,b}, Lei Jin^e, Kefeng Dai^d, Chaobin Mao^d, Sanzhong Wu^d, Rongwei Zhang^g, Jinsong Yang^g, Jianguo Ying^g, Jiajie Fan^{a,b,c,*}, Hongping Ma^{a,b,c,*}, Guoqi Zhang^f

^a Institute of Wide Bandgap Semiconductors and Future Lighting, Academy for Engineering & Technology, Fudan University, Shanghai 200433, China

^b Shanghai Research Center for Silicon Carbide Power Devices Engineering & Technology, Fudan University, Shanghai 200433, China

^c Institute of Wide Bandgap Semiconductor Materials and Devices, Research Institute of Fudan University in Ningbo, Zhejiang 315327, China

^d Department of Equipment Research for Wide Bandgap Semiconductor, Jihua Laboratory, Foshan 528200, China

^e 48th Research Institute of China Electronics Technology Group Corporation, Changsha 410111, China

^f EEMCS Faculty, Delft University of Technology, 2628 Delft, the Netherlands

^g Ningbo Xinsheng Medium Voltage Electrical Appliance Co., Ltd., Zhejiang 315032, China

ARTICLE INFO

Keywords:

4H-SiC homoepitaxial layer
CVD reactor
Susceptor rotation speed
Quality
Defects

ABSTRACT

In this work, 4H-SiC homoepitaxial layers were grown on 4° off-axis substrates at different susceptor rotation speeds by using a hot-wall horizontal CVD reactor. The effect of different susceptor rotation speed on the quality of 4H-SiC epitaxial layers in terms of thickness, thickness uniformity, crystallinity, surface morphology and morphological defects was investigated via Fourier transform infrared spectroscopy (FTIR), high-resolution X-ray diffraction (XRD), atomic force microscopy (AFM), confocal differential interference contrast microscopy (CDIC), ultra-violet photo-luminescence spectroscopy (UV-PL), scanning electron microscopy (SEM), and micro-Raman spectroscopy, respectively. A flow field simulation was performed to explain the impact of susceptor rotation speed on the film deposition. The FTIR results suggested that the susceptor rotation speed could be an important factor to adjust thickness uniformity and deposition rate. The XRD patterns showed that crystallinity was independent of the susceptor rotation speed. The surface morphology can be improved by changing the susceptor rotation speed. According to CDIC scans, the down-fall related defects were reduced through the increase in the susceptor rotation speed. The origin of down-fall related defects was interpreted by Raman spectroscopy and speculative models. To sum up, the susceptor rotation speed is a crucial factor in increasing growth rate and improving uniformity. Also, the faster susceptor rotation speed helps reduce the number of down-fall related defects in the hot-wall CVD reactor.

1. Introduction

Silicon carbide (SiC) is a very desirable semiconductor material that is extensively applied in high-power, high-temperature, and high-frequency electronic devices due to its unique characteristics[1–3]. SiC is recognized to crystallize in nearly 250 different polytypes, the most common ones are the 2H, 3C, 4H, and 6H structures. Among those polytypes, 4H-SiC has the superior advantages in terms of electrical, physical and chemical properties, such as high electron saturation velocity, wide band-gap, easy-to-grow ingots at the reasonable rates, high

power conversion efficiency, and outstanding thermal conductivity [4–7]. All these characteristics make 4H-SiC a preferable material for next-generation high-voltage power devices[8,9]. Chemical vapor deposition (CVD) has recently become a common technology to grow 4H-SiC epitaxial layers on homogeneous substrates owing to its film uniformity and controllable growth process. This method enables to realize the high-quality homoepitaxial growth of the drift layer on 4H-SiC substrates in the power electronic devices with good surface morphology, preferable thickness uniformity, desirable dopant distribution, and excellent crystallinity, which are essential for the

* Corresponding authors at: Institute of Wide Bandgap Semiconductors and Future Lighting, Academy for Engineering & Technology, Fudan University, Shanghai 200433, China

E-mail addresses: jiajie_fan@fudan.edu.cn (J. Fan), hpma@fudan.edu.cn (H. Ma).

<https://doi.org/10.1016/j.mtcomm.2024.108037>

Received 16 October 2023; Received in revised form 19 December 2023; Accepted 2 January 2024

Available online 5 January 2024

2352-4928/© 2024 Elsevier Ltd. All rights reserved.

development of high-performance power electronic devices[10–15].

It has been shown that 4H-SiC homoepitaxial growth can be carried out on the off-axis substrates in the “step-flow growth mode” so as to enhance polytype stability[16]. In addition, low-angle off-axis substrates (the off-axis angle with [0001] and [112(–)0] directions is 4°) are suitable for commercial homoepitaxial growth because of the following reasons. One is that it is conducive to reduce the cost of material, for example, more pieces of 4° off-axis substrates can be sliced than those of larger off-axis angle substrates from the SiC ingots [17,18]. Another is that the basal plane dislocations (BPDs) on the substrate surface can be reduced by using 4° off-axis substrates[19]. Besides the impact of the substrate during the growth, the use of chlorine-based gas [10,20] and in-situ etching[21] is beneficial for the fast growth of 4H-SiC epi-layer with smooth surface and good uniformity on the off-axis substrate. It is found that C/Si ratio has a great influence on the crystallinity, growth rate, and surface roughness during the CVD epitaxial growth[22]. It has also been demonstrated that suitable Cl/Si ratio can suppress the 3C-inclusion[23], eliminate triangle defects[24] and exert impact on the surface mobility[25]. Various experiments on 2-inch and 4-inch substrates have revealed that the surface morphology can be improved with an increase of growth temperature[26]. Moreover, the aluminum dopant concentration during the growth on 3-inch substrates accounts for the gas flow state, rising with the increase in the hydrogen flow rate[27].

With the booming development of power devices and the enlargement of SiC ingots in recent years, the large-size (the diameters of 150 mm or more) 4H-SiC substrates have attracted a lot of attention from researchers, becoming the mainstream in the low-cost manufacturing of power appliances. For example, Masumoto *et al.*[28] produced epitaxial layers on 4H-SiC substrates with 150 mm diameters by using a CVD deposition system. In particular, the effect of the C/Si ratio on the surface morphology, surface defects density, and thickness and carrier concentration uniformity was studied. Li *et al.*[29] investigated the common surface defects in 4H-SiC homoepitaxial layers with 150 mm diameters. According to the results, triangular defects were reduced with the increase in the growth temperature, and a step-bunching free epitaxial layer, on the other hand, was obtained by decreasing the growth temperature. Yu Saitoh *et al.*[30] have proposed the high-uniformity epitaxial growth mechanism to produce C-face 4H-SiC epitaxial layers with 150 mm diameters by adjusting the growth parameters. Zhao *et al.*[31] used the 4° off-axis 150 mm diameter substrates to form trenches for fabricating the super-junction power devices, and particular attention was paid to the influence of growth pressure and Cl/Si ratio on the epi-layer distribution in the trenches and the filling efficiency of CVD method. Since the size of the substrate gradually increased, the corresponding diameter of the CVD reactor needed to be expanded, which led to the uneven temperature and flow fields compared to a small-size reactor. Furthermore, the CVD homoepitaxial growth strongly relied on the high temperature reaction between the reactants and flow state in the CVD reactor[19,32–34]. In this case, parameters such as the inject gas flow ratio, and inject gas-flow rate that affect the flow field in the CVD reactor are important factors during the epitaxial growth process, especially for the substrates with large diameters like 150 mm or more. However, during the 4H-SiC growth process, a lot of studies mainly focus on epitaxial parameters such as growth temperature of reactor, cavity pressure, gas ratio of reactant, influence of the etching by carrier gas, and even substrate itself. To date, limited works have been conducted on the effect of susceptor rotation speed on the quality of epitaxial layer and its influence on flow field based on horizontal hot-wall CVD reactor.

In view of the above, this work aims to systematically study the effect of the susceptor rotation speed on the quality of epitaxial layers grown on 150 mm 4° off-axis 4H-SiC substrates via CVD method. Furthermore, a flow field simulation of the reactor has been built for better understanding the influence of susceptor rotation speed on the film deposition. Based on the experimental results, epitaxial layer thickness,

morphological defects, surface morphology, and crystallinity will be discussed.

2. Experimental methods

2.1. Apparatus and film deposition

The 4H-SiC homoepitaxial layer was deposited in a low-pressure home-made horizontal hot-wall CVD reactor using a SiHCl₃(Trichlorosilane, TCS) + C₂H₄ + H₂ system. Fig. 1(a) displays a schematic diagram of the CVD apparatus, in which a graphite reaction chamber is surrounded by the insulation material inside a quartz tube. The quartz tube and induction coil have the double layers, and the hollow areas in their middles are filled with water as a coolant. The rotational susceptor which carries the 4H-SiC substrates at the center area of the down-graphite heater can be levitated and rotate by using H₂ as the driving gas. In this gas-foil-rotation technology, the rotational speed of the substrate can be adjusted by changing the flow rate of H₂.

The n-type 4H-SiC substrates with diameter of 150 mm used in this work had Si-terminated (0001) faces with 4° off-axes oriented toward the [112(–)0] crystal direction. TCS and ethylene (C₂H₄) were introduced into the reactor as the Si and C sources, respectively. H₂ served as the dilution, carrier, and etching gas. Before the reactor reached the growth temperature, the 4H-SiC substrate was etched in an H₂ atmosphere for 10 min. Within the whole experiment, the H₂ carrier flow rate and C/Si ratio were fixed at 120 slm and 1.2, respectively, under the chamber pressure of 75 Torr. The epitaxial growth lasted 30 min, and the growth temperature was fixed at 1610 °C in these experiments.

2.2. Simulation setup

The simulation model of the horizontal hot-wall CVD reactor can be seen in Fig. 1(b). The dimensions (length, height, and width) were exactly the same as those of the real apparatus displayed in Fig. 1(a). The professional software (COMSOL Multiphysics) was used in simulation. Fig. 1(b) depicts three groups of gas vents in the reactor. Two groups of side gas vents contained four vents on the left and right sides of the gas inlet area, and another group included fourteen vents located at the center of the gas inlet area. All three groups of vents had the same inlet velocity, and the outlet gas vent was under a zero pressure. In the reality, the amounts of C₂H₄ and TCS (in sccm) were negligible compared to that of H₂ (in slm) in the total flow rate. For this reason, only H₂ will be considered in the reactor domain during the simulation process.

The simulation consisted in the qualitative analysis of the flow field state in the reactor. Therefore, for the model simplicity and the simulation convergence, it was assumed that: (1) the flow state was laminar, and the flow speed at the surface of the substrate was zero; (2) the flow field was considered to be in steady, isothermal and incompressible state; (3) the density, conductivity, and dynamic viscosity of the fluid were constant. According to these assumptions, the gas transport can be mathematically described by the Navier-Stokes equation and continuity equation[35], respectively, as follows:

$$\rho (\mathbf{u} \cdot \nabla) \mathbf{u} = \nabla \cdot [-p\mathbf{I} + \mu(\nabla \mathbf{u} + (\nabla \mathbf{u})^T)] + \mathbf{F} \quad (1)$$

$$\rho \nabla \cdot (\mathbf{u}) = 0 \quad (2)$$

where ρ is the gas density, \mathbf{u} is the gas velocity, p is the pressure, μ is the fluid dynamic viscosity, T is the temperature, and \mathbf{F} is the volume force of the fluid.

2.3. Characterization

According to the above parameters, a total of four comparative epitaxial growth processes at different susceptor rotation speeds were conducted. The epitaxial layer thickness of all samples onto the

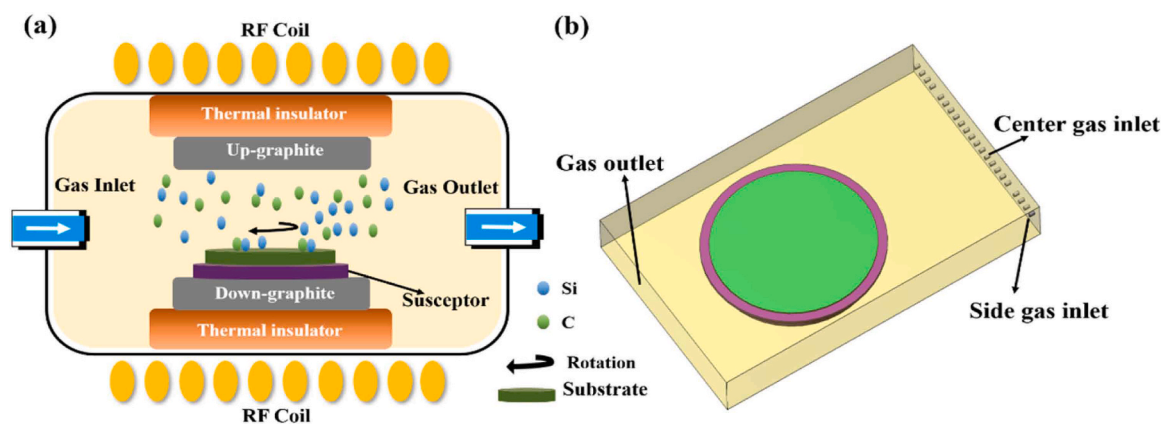


Fig. 1. (a) Schematic diagram of the cross-section of the CVD apparatus; (b) structure of a horizontal hot-wall CVD reactor in simulation.

substrates was determined via Fourier transform infrared spectroscopy (FTIR, ThermoFisher Scientific). During the thickness measurement, the edge exclusion was 5 mm. Various characterization methods were then adopted for surface analysis. Among them, atomic force microscopy (AFM, Bruker) was applied to characterize the surface roughness and morphology. The crystal structures and crystallinity degrees were analyzed via high-resolution X-ray diffraction (XRD, Bruker AXS) using Cu K α radiation (40 kV, 40 mA, $\lambda = 1.54 \text{ \AA}$) in the 2θ - ω scan range from 5° to 65° and by recording the omega rocking curves. Besides, confocal differential interference contrast microscopy (CDIC, Lasertec SICA88) was used to measure the morphological defect number. Ultra-violet photo-luminescence (UV-PL) spectroscopy and scanning electron microscopy (SEM) were also employed to detect the defects. The micro-Raman spectroscopy analysis using a 532 nm green-diode laser (5 mW) was performed as well.

3. Results and discussion

3.1. Thickness

The even distribution or good uniformity of a deposited film is important to produce high-quality epitaxial wafers. To obtain the information about the 4H-SiC film distribution at different susceptor rotation speeds, the surface of each sample was examined via FTIR. In particular, 57 points were scanned inside the wafer to draw a thickness map, and two test lines (one perpendicular to the gas inlet direction and the other one parallel to it) were traced along the radial directions of the wafer through a total of 17 points, as shown in Fig. 2(a), to determine the radial distribution of the epitaxial wafer thickness.

The average thickness and uniformity of the samples were assessed by using the mean value ($\bar{x}(\dots)$) and standard deviation/mean (σ/\bar{x}) value of 17 points according to the formulae below:

$$\bar{x} = \frac{\sum_{i=1}^{17} x_i}{17} \quad (3)$$

$$\sigma / \bar{x} (\%) = \frac{\sqrt{\frac{\sum_{i=1}^{17} (x_i - \bar{x})^2}{16}}}{\bar{x}} \quad (4)$$

The corresponding results at different susceptor rotation speeds are plotted in Fig. 2(b). The average thickness increased from $14.77 \mu\text{m}$ to $16.22 \mu\text{m}$ with the increase in susceptor rotation speed from 0 to 60 rpm. Since all samples had the same growth time, the average thickness represented the growth rate as well. Previous studies have reported that the relationship $\text{GR} \propto 1/\partial \propto (\omega P)^{1/2}$ [36–40] stems from the boundary layer theory as mentioned above, where GR is the growth rate, ∂ is the thickness of the boundary layer, ω is the susceptor rotation speed, and P is the pressure in the reactor. It is noteworthy that though the pressure was fixed during the experiments, the growth rate was proportional to the susceptor rotation speed, which was in accordance with the data in Fig. 2(b). Besides the boundary theory, the susceptor was driven by the hydrogen gas at room temperature for rotation, and the volume of the gas increased with the increase of the rotational speed, which would have led to a slight decrease of the temperature inside the reactor

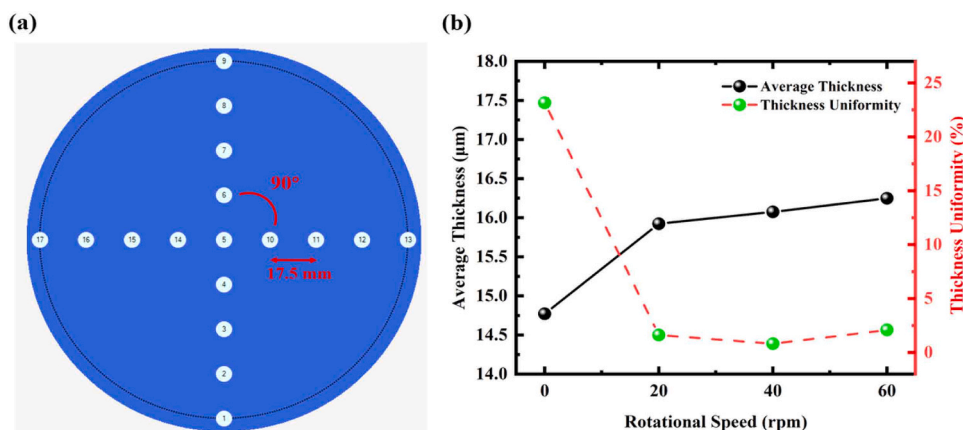


Fig. 2. (a) 17 test points acquired for FTIR analysis; (b) average thickness and thickness uniformity for all samples.

chamber. A relatively low temperature upon the 4H-SiC film growth results in the high growth rate, and the impact of hydrogen etching on the film growth becomes weakened at lower temperatures[34,41]. In this case, the growth rate or thickness rises up with the increasing susceptor rotation speed. Also, the worst thickness uniformity (23.16%) was enriched at the fixed susceptor (0 rpm), and the best thickness uniformity was 0.82% at 40 rpm, as shown in Fig. 2(b). Therefore, adjusting the susceptor rotation speed could be an approach to achieve the better thickness uniformity for the horizontal hot-wall CVD reactor.

The thickness maps, radial thickness distributions, and simulation results at different rotational speed is shown in Fig. 3. As it can be seen from Fig. 3(a1) and 3(a2), the thickest deposition part on the substrate is the edge region near the gas inlet vent, and the film thickness has decreased from 22.44 μm to 9.01 μm along the gas flow direction. It has the linear growth profile from gas inlet vent to gas outlet vent without rotation of susceptor, which lead to the worst uniformity as mentioned

above. In addition, the thickness along the horizontal direction exhibited only a slight fluctuation. These phenomena can also be explained in the context of the boundary layer theory[38]. When the susceptor is kept stationary, the boundary layer thickness is minimal at the substrate edge near the gas inlet, and the diffusive flux of the reactants which directly impact on the deposition rate is inversely proportional to the boundary layer thickness. According to Fig. 3(a3), the stationary susceptor exerts no influence on the flow field and causes no flow disturbance on the surface of the substrate compared to other rotating susceptors. Under such conditions, the parts of the reactor, in which the diffusive fluxes of reactants are maximal and grant the strongest driving force for the surface reactions, correspond to the substrate edges closest to the gas inlet vent.

In Fig. 3(b1)– 3(d1), the orange color denotes the thinner film on the edge of the wafer at the rotational speed of 20 rpm. The blue and dark green referring to a thicker film area appeared on the edge of the wafer

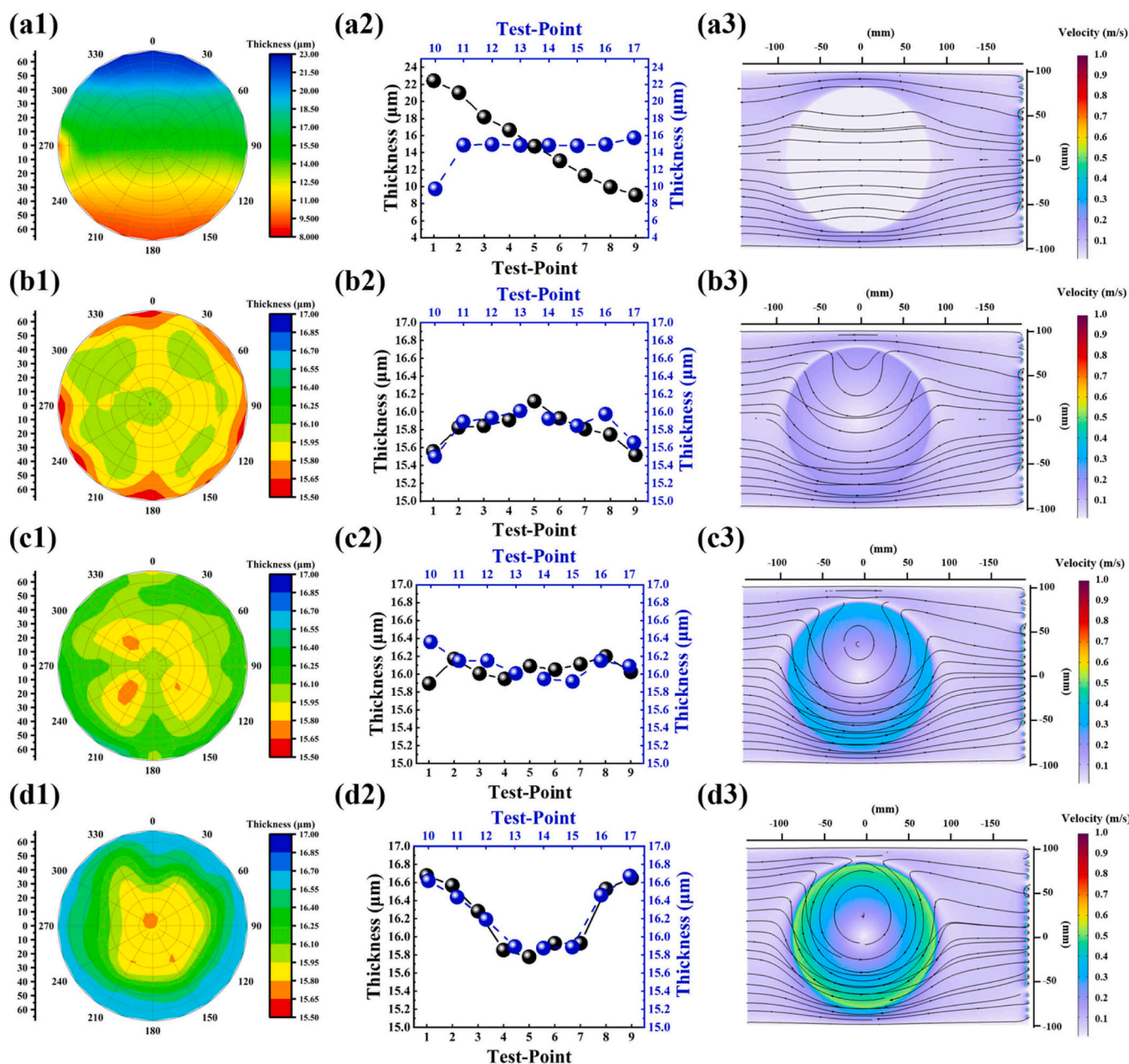


Fig. 3. Thickness maps of the epitaxial wafers, 17 test-point thickness measurements and flow field simulation inside the reactor at the rotational speed of (a1-a3) 0 rpm; (b1-b3) 20 rpm; (c1-c3) 40 rpm; (d1-d3) 60 rpm.

as the susceptor rotation speed increased. The thinner film areas corresponding to light green, orange, yellow and red colors shrunk gradually and moved toward the center of the wafer as the susceptor rotation speed reached 60 rpm. In Fig. 3(b2)– 3(d2), the radial distributions of the film thickness are displayed as the “∩”, “~” and “U” shapes at 20, 40 and 60 rpm, respectively, and the edge of the wafer becomes thicker. In Fig. 3(b3)– 3(d3), the brighter color represents the higher flow rate region in the reactor. Once the susceptor rotation speed increased from 20 to 60 rpm, the brighter color regions gradually moved from the edge to the center of susceptor and a swirling turbulence gradually showed up above the susceptor. The flow speed at the edge of the wafer rose with the increase in the susceptor rotation speed. According to these simulation and experimental results, it is obvious that the increase of the

susceptor rotation speed alters the flow field inside the reactor, and the flow speed is gradually enhanced from the edge toward the center of the wafer. Besides that, a growing flow speed difference between the edge and the center of the wafer with the scaling up susceptor rotation speed is the main reason that more and more reactants spread on the edge of the wafer. Based on the boundary layer theory, the higher flow velocity yields a thinner boundary layer[38]. Thus, the closer it is to the edge of the wafer, the higher the deposition rate, which is in accordance with Fig. 3(b2)– 3(d2).

3.2. Crystallinity and morphology

To confirm whether the susceptor rotation speed affects the

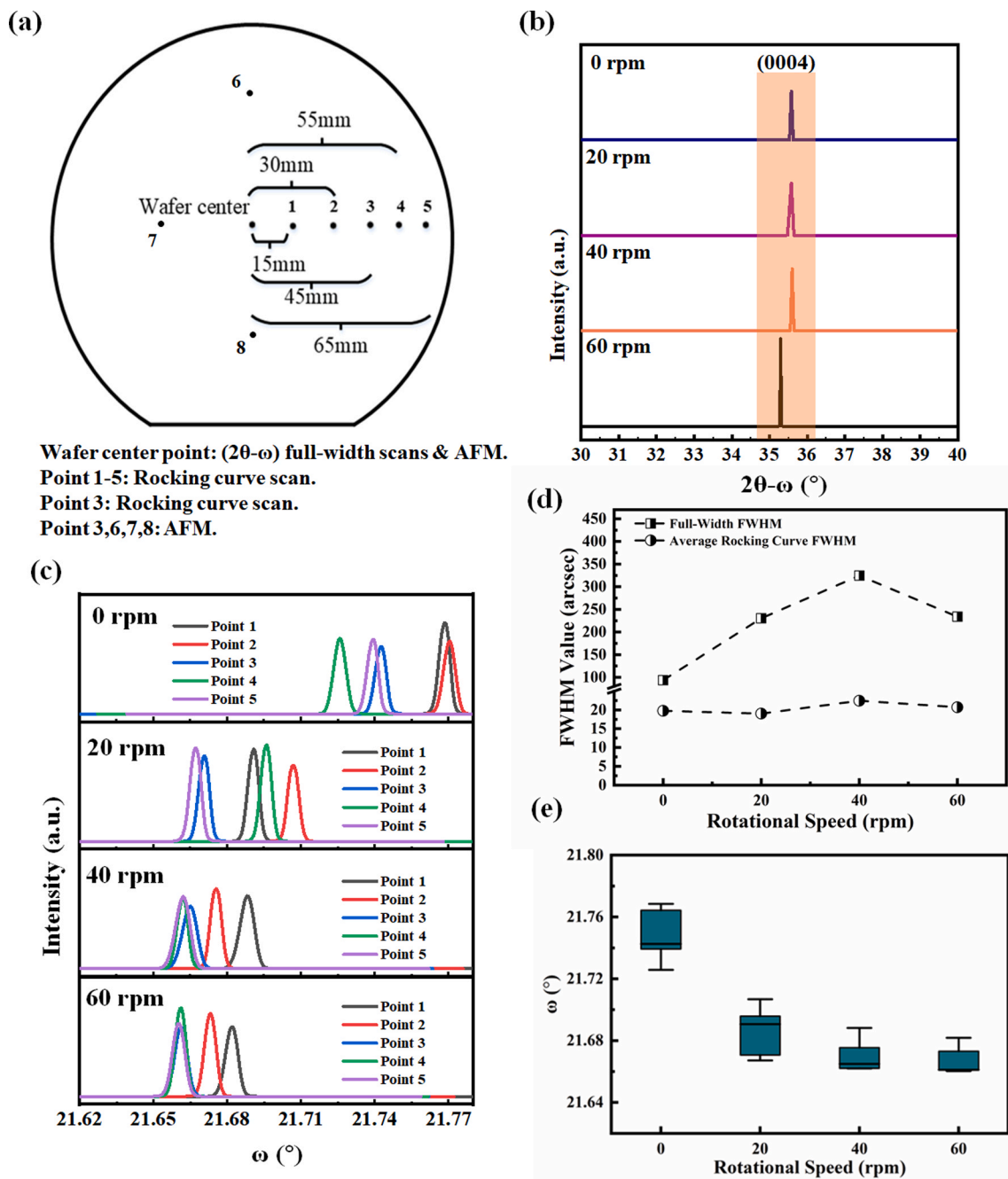


Fig. 4. (a) Location of test points in the epitaxial wafer for XRD and AFM analysis; (b) XRD full-width patterns of the center area of 4H-SiC epitaxial wafer at various rotational speeds; (c) XRD rocking curve at test points 1–5 at various rotational speeds; (d) FWHMs, rocking curves and surface roughness values of 4H-SiC epitaxial wafer at various susceptor rotation speeds; (e) peak locations of the rocking curve at different susceptor rotation speeds.

crystallinity of the epitaxial film or not, the HRXRD analysis of the epitaxial wafer was afterward performed (see Fig. 4(a)). In particular, the full width was measured at the wafer center, and the rocking curve was acquired along the radial direction of the wafer at points 1–5 to further observe the influence of susceptor rotation speed on epitaxial wafer crystallinity.

Fig. 4(b) and (c) depict the XRD patterns of the epitaxial film at different susceptor rotation speeds. Fig. 4(b) shows the typical XRD full-width scans in the range of 30° to 40° at the epitaxial wafer center. In all cases, the high-intensity diffraction peaks around 35.6° were observed without any spurious peaks due to the 4° off-axis epitaxial wafer diffraction from the (0004) plane of the high-quality 4H-SiC single crystal, which was similar to Ref. [42]. Fig. 4(c) depicts the rocking curves from 0 to 60 rpm along the radial direction of the epitaxial wafer, and those measured with a medium incident angle around 21.7° (Fig. 4(e)) are the same as the typical XRD spectra of 4H-SiC single crystals [15]. In addition, Fig. 4(d) demonstrates the relationship between the full width at half-maximum (FWHM) value of the epitaxial wafer and the susceptor rotation speed. The higher FWHM values represented the worse quality of crystal, and the epitaxial wafer center at 0 rpm exhibited the smallest full-width FWHM value of 93.6", thus proving the better crystallinity compared to other samples at different rotational speeds. The worst crystallinity (full-width FWHM = 324.8") was obtained at the center of the epitaxial wafer at 40 rpm. Moreover, the rocking curve at these test points remained steady while changing the speed from 0 to 60 rpm. Earlier reports affirmed that crystal defect density, crystal strain in the substrate, and C/Si ratio have huge impact on epitaxial film's FWHM value and thus crystallinity [22,43,44]. Based on above facts and results, although better crystallinity at wafer center of 0 rpm than other sample of speed, the crystallinity of whole wafer was almost independent of rotational speed within the experimental range.

In order to confirm the surface quality of 4H-SiC epitaxial layers grown at different susceptor rotation speeds, the surface roughness (Ra) was measured at five monitoring points with a 5 μm x 5 μm area, as shown in Fig. 4(a). The surface roughness values of these five points can be seen in Table 1, and the average values for 0 rpm, 20 rpm, 40 rpm and 60 rpm are 0.2086 nm, 0.142 nm, 0.159 nm and 0.107 nm, respectively. Figs. S1(a)–S1(d) displayed the AFM images highlighting the 2D and 3D surface morphologies of the 4H-SiC films at the changing susceptor rotation speed.

On the whole, with the increase of the susceptor rotation speed in the experimental range, the value of surfaces roughness varied from 0.2086 nm to 0.107 nm. Therefore, the above results indicated that, except for process parameters such as the growth temperature, C/Si ratio and in-situ etching [18,22,45,46], the surface morphology can be improved with the increase of susceptor rotation speed within the experimental range.

3.3. Morphological defects

The main morphological defects include particles, triangles, downfall related defects (DF and DF triangles), and carrots [47]. The influence of the susceptor rotation speed on these defects can be seen in Fig. 5(a). Except for downfall related defects, the particle, triangle, and carrot defect are not sensitive to the effect of susceptor rotation speed. The particle defects are generally related to cleanliness of the substrate,

Table 1
RMS values for samples at different rotational speed.

Rotational Speed (rpm)	Up (nm)	Left (nm)	Right (nm)	Center (nm)	Down (nm)	Average (nm)
0	0.192	0.185	0.291	0.197	0.178	0.2086
20	0.148	0.156	0.129	0.148	0.129	0.142
40	0.127	0.167	0.246	0.123	0.132	0.159
60	0.108	0.106	0.107	0.106	0.108	0.107

reactor chamber, and environment of the laboratory room [48]. Since these factors remained almost unchanged in this study, there was no significant alteration in this kind of defects. The impact of susceptor rotation speed on the number of triangle defects was negligible as well. Triangle defects are mainly controlled or suppressed by other parameters such as growth temperature and C/Si ratio [29]. The carrot defects also exhibited no obvious variation with the change in the susceptor rotation speed. The origins of the carrot defects like threading screw dislocations and basal plane dislocations within the substrate have been reported in many researches [49,50]. An enormous decrease in carrot defect density can be obtained by optimizing the buffer layer and in-situ etching conditions prior to the epitaxial growth [51]. In this situation, the number of carrot defect largely depends on the quality of the substrate. Since the substrate and buffer layer during the experiments were processed from the same ingot and fixed parameters, the carrot defect data Fig. 5(a) were consistent with the earlier studies as mentioned above.

Concerning the total downfall related defects (the sum of DF and DF triangles), their amount decreased with the increase of the rotational speed, as seen in Fig. 5(b). The total number of downfall related defect was 233, 137, 105, and 87 when the rotational speed at 0, 20, 40, and 60 rpm, respectively. Besides, these DF related defects were randomly distributed at different susceptor rotation speeds (Fig. 5(c1)–5(c4)). It is well known that multiple by-products are attached to the walls of the CVD reactor during the growth of 4H-SiC films [52]. Therefore, the mentioned surface defects could be associated to the unwanted by-products deposited inside the reactor and falling onto the wafer during the epitaxial process. Some by-products on the wafer formed DF defects and some generated DF-triangle defects. To clarify the origin of both downfall related defects, the SEM image of a DF-triangle defect and the UV-PL image of a DF defect (Figs. 6(a) and 6(c), respectively) were inspected. As shown in the SEM images in Figs. 6(a) and 6(b), the DF-triangle defect had a prominent triangular shape with a circular particle located at the apex of the triangle. The by-products fallen onto the wafer prevented the 4H-SiC step flow growth and formed the triangular region behind it [53]. According to previous studies, most by-products that cause the DF-triangle defects at the substrate/epitaxial interface [53,54] precipitate onto the wafer at the initial stage of the growth. Since all experiments in this study were done conforming to the same procedure from the beginning to the susceptor rotation speed stabilization, this explained the irregular variety in DF-triangle defects with the increasing susceptor rotation speed. On the other hand, the UV-PL image of the DF defect (Fig. 6(c)) reveals a black dot which resembles the by-product directly hitting the thin film. Unlike those downfall products that form DF triangles at the earlier stage, these DF defects were introduced near the end of the growth process. The reason why the number of DF defects decreases with the increase in the susceptor rotation speed will be discussed later. To further investigate the by-products that cause DF-triangle and DF defects, the Raman spectroscopy measurement was conducted. The Raman spectra acquired at the 4H-SiC matrix, the DF-triangle dotted area, and the DF defect dotted zone are shown in Figs. 6(a) and 6(c). Fig. 6(d) displays the micro-Raman spectra collected in the mentioned points in the range between 650 and 1100 cm⁻¹, in which the peaks at 776.8, 776.98, 797.9, 964.52, 972.3 and 973.5 cm⁻¹ were clearly distinguished. According to the literature [55], the spectral bands at 776, 796 and 964 correspond to the folded modes of the transverse optic branches (FTO (2/4) and (0)) and the longitudinal optical branch (FLO(0)) for 4 H-SiC, respectively. The features at 796 and 972 cm⁻¹ are ascribed to FTO(0) and FLO(0) related modes of 3C-SiC [55], respectively. Therefore, the dotted areas in the SEM and UV-PL images might be 3C-SiC crystal precipitates onto the wafer surface.

The higher susceptor rotation speed of susceptor in the horizontal hot-wall CVD reactor seems to be beneficial for the DF defect reduction. Similar results were also demonstrated for the upper gas inlet, the hot wall, and the vertical CVD reactor [56]. The reduction of DF defects can

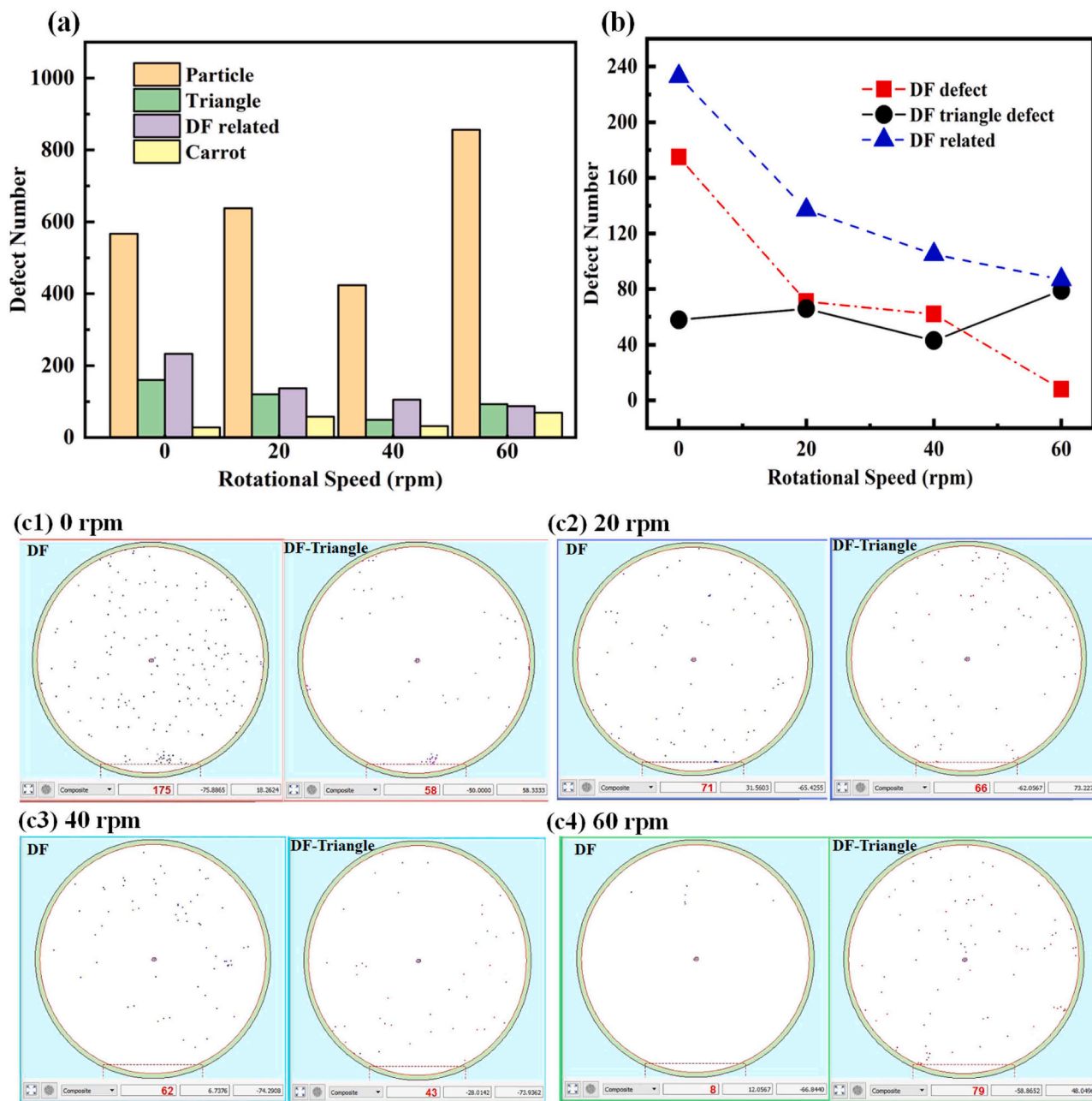


Fig. 5. (a) Histogram reflecting the morphological defects at different rotational speeds of susceptor; (b) number of DF related defects at different rotational speeds of susceptor; (c1)-(c4) surface defect distribution within the epitaxial layer, including DF and DF-triangle defects at the rotational speeds of 0, 20, 40, and 60 rpm.

be explained in the context of two possible models. One model is shown in Fig. 7 whereby the rotating susceptor alters the flow field and creates a difference between the flow speeds on the wafer, thus causing a swirling turbulence as a protective shield above the surface of the wafer as mentioned in Fig. 3. This swirling interplays with the inlet gas to push out some 3C-SiC crystals outside the top of the wafer. When the susceptor is kept stationary, it is highly likely that by-products or 3C-SiC crystals will directly hit the surface of the wafer, and the feasible DF defect content will be highest at the rotational speed of 0 rpm. Another possible explanation is that the fast gas flow along with the centrifugal force eliminate the particles that form the DF defects on the surface of the wafer [57]. The DF defect reduction can thus be achieved through the increase in the susceptor rotation speed from 0 to 60 rpm for the horizontal hot-wall CVD reactor during the deposition process.

4. Conclusions

In this work, 4H-SiC homoepitaxial layers were grown on 4° off-axis substrates by using the hot-wall horizontal CVD reactor at four susceptor rotation speeds upon the film growth. The thickness, thickness uniformity, crystallinity, surface morphology and morphological defects of the 4H-SiC homoepitaxial wafer under different susceptor rotation speeds were investigated via FTIR, XRD, AFM and CDIC, respectively. A flow field simulation was also performed to better understand the impact of susceptor rotation speed on the thickness variation of epitaxial wafer. It was found that the deposition rate or average thickness increases from 14.77 μm to 16.22 μm as the susceptor rotation speed increase, and the closer was it to the edge of wafer the higher was the deposition rate. The layer thickness was more uniform from 23.16% to the lowest 0.82% when the growth was accompanied by the rotation of susceptor. The surface morphology can be improved by increase the rotation speed of

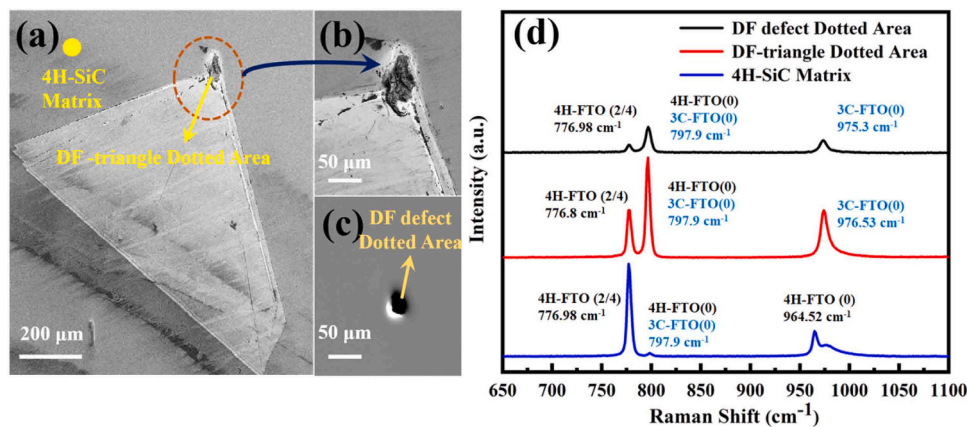


Fig. 6. (a) SEM image of DF triangle defect; (b) the magnified view of the DF-triangle dot area; (c) UV-PL image of DF defect; (d) micro-Raman spectra of DF defect dotted area, DF-triangle dotted area, and 4H-SiC matrix.

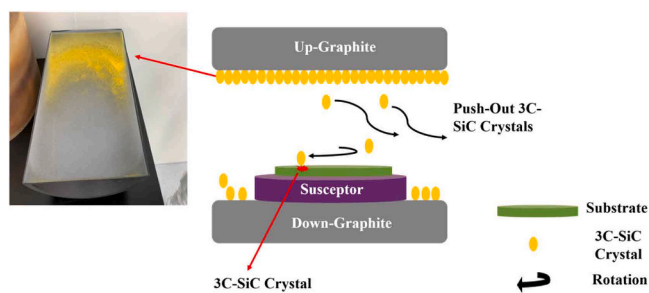


Fig. 7. Model of rotational susceptor for the reduction of DF defects.

susceptor. However, the crystallinity was independent of the susceptor rotation speed. The number of morphological defects was obtained and analyzed as well. The result showed that only down fall related defects decreased with the increase of the susceptor rotation speed, and the number of down fall related defects reduced to 87 as the susceptor rotation speed reached to 60 rpm, whereas no remarkable difference was observed for other morphological defects at any susceptor rotation speed. The dotted area of DF related defects might be 3C-SiC fallen down onto the surface of the wafer. Besides, two possible reasons were proposed to explain the decrease in DF related defects. Therefore, whether the susceptor rotate or not, it has little effect on the crystallinity of 4H-SiC epitaxial layer based on above experiments. The rotational susceptor in the reactor is beneficial for obtain high uniformity and low surface roughness 4H-SiC epitaxial layer. Also, the susceptor rotation speed is a critical parameter to control the number of DF related defects.

CRedit authorship contribution statement

Ying Jianguo: Resources. **Zhang Guoqi:** Funding acquisition, Project administration, Resources, Supervision. **Zhang Rongwei:** Resources. **Yang Jinsong:** Resources. **Ma Hongping:** Funding acquisition, Project administration, Supervision, Validation. **Gu Lin:** Data curation, Formal analysis, Investigation, Validation. **Jin Lei:** Investigation, Writing – review & editing. **Tang Zhuorui:** Data curation, Formal analysis, Methodology, Writing – original draft. **Wu Sanzhong:** Resources, Validation. **Fan Jiajie:** Funding acquisition, Project administration, Supervision. **Dai Kefeng:** Data curation, Validation. **Mao ChaoBin:** Resources, Validation.

Declaration of Competing Interest

The authors declare that they have no known competing financial

interests or personal relationships that could have appeared to influence the work reported in this paper.

Data availability

Data will be made available on request.

Acknowledgments

This work are supported by the Science and Technology Innovation Plan of Shanghai Science and Technology Commission (No. 21DZ1100800 and 23ZR1405300), National Natural Science Foundation of China (52275559), and Shanghai Pujiang Program (2021PJD002).

Appendix A. Supporting information

Supplementary data associated with this article can be found in the online version at [doi:10.1016/j.mtcomm.2024.108037](https://doi.org/10.1016/j.mtcomm.2024.108037).

References

- [1] T. Kobayashi, K. Harada, Y. Kumagai, et al., Native point defects and carbon clusters in 4H-SiC: a hybrid functional study [J], *J. Appl. Phys.* 125 (12) (2019) 125701.
- [2] S. Wei, Z. Yin, J. Bai, et al., The structural and electronic properties of carbon-related point defects on 4H-SiC (0001) surface [J], *Appl. Surf. Sci.* 582 (2022) 152461.
- [3] K. Fukuda, A. Kinoshita, T. Ohyanagi, et al., Influence of processing and of material defects on the electrical characteristics of SiC-SBDs and SiC-MOSFETs [C], *Mater. Sci. Forum* (2010) 655–660.
- [4] M. Soueidan, G. Ferro, A vapor–liquid–solid mechanism for growing 3C-SiC single-domain layers on 6H-SiC (0001) [J], *Adv. Funct. Mater.* 16 (7) (2006) 975–979.
- [5] S. Leone, F.C. Beyer, A. Henry, et al., Chloride-based CVD of 3C-SiC epitaxial layers on 6H (0001) SiC [J], *Phys. Status Solidi (RRL)–Rapid Res. Lett.* 4 (11) (2010) 305–307.
- [6] X. Qian, P. Jiang, R. Yang, Anisotropic thermal conductivity of 4H and 6H silicon carbide measured using time-domain thermoreflectance [J], *Mater. Today Phys.* 3 (2017) 70–75.
- [7] V. Soler, M. Cabello, M. Berthou, et al., High-voltage 4H-SiC power MOSFETs with Boron-doped gate oxide [J], *IEEE Trans. Ind. Electron.* 64 (11) (2017) 8962–8970.
- [8] F. Roccaforte, P. Fiorenza, G. Greco, et al., Emerging trends in wide band gap semiconductors (SiC and GaN) technology for power devices [J], *Microelectron. Eng.* 187 (2018) 66–77.
- [9] K. Fukuda, D. Okamoto, M. Okamoto, et al., Development of ultrahigh-voltage SiC devices [J], *IEEE Trans. Electron Devices* 62 (2) (2014) 396–404.
- [10] S. Leone, A. Henry, E. Janzén, et al., Epitaxial growth of SiC with chlorinated precursors on different off-angle substrates [J], *J. Cryst. Growth* 362 (2013) 170–173.
- [11] T. Kimoto, S. Nakazawa, K. Hashimoto, et al., Reduction of doping and trap concentrations in 4H-SiC epitaxial layers grown by chemical vapor deposition [J], *Appl. Phys. Lett.* 79 (17) (2001) 2761–2763.
- [12] Y. Sharma, H. Jiang, C. Zheng, et al., Impact of design and process variation on the fabrication of SiC diodes [J], *J. Semicond.* 39 (11) (2018) 114001.

- [13] J. Chen, M. Guan, S. Yang, et al., Characterization of epitaxial layers grown on 4H-SiC (0 0 0–1) substrates [J], *J. Cryst. Growth* 604 (2023) 127048.
- [14] Z. Tang, L. Gu, H. Ma, et al., Study on the surface structure of N-Doped 4H-SiC homoepitaxial layer dependence on the growth temperature and C/Si ratio deposited by CVD [J], *Crystals* 13 (2) (2023) 193.
- [15] Z. Shen, F. Zhang, X. Liu, et al., Influence of H₂ treatment on the surface morphology of SiC with different wafer orientation and doping [J], *J. Cryst. Growth* 607 (2023) 127105.
- [16] A. Itoh, H. Akita, T. Kimoto, et al., High-quality 4H-SiC homoepitaxial layers grown by step-controlled epitaxy [J], *Appl. Phys. Lett.* 65 (11) (1994) 1400–1402.
- [17] X. Li, J. Hassan, O. Kordina, et al., Surface preparation of 4 off-axis 4H-SiC substrate for epitaxial growth [C], *Mater. Sci. Forum* (2013) 225–228.
- [18] S. Leone, H. Pedersen, A. Henry, et al., Improved morphology for epitaxial growth on 4 off-axis 4H-SiC substrates [J], *J. Cryst. Growth* 311 (12) (2009) 3265–3272.
- [19] K. Wada, T. Kimoto, K. Nishikawa, et al., Epitaxial growth of 4H-SiC on 4 off-axis (0 0 0 1) and (0 0 0 1) substrates by hot-wall chemical vapor deposition [J], *J. Cryst. Growth* 291 (2) (2006) 370–374.
- [20] H. Das, S.G. Sunkari, T. Oldham, et al., High uniformity with reduced surface roughness of chloride based CVD process on 100mm 4 off-axis 4H-SiC [C], *Mater. Sci. Forum* (2012) 93–96.
- [21] L. Dong, G. Sun, J. Yu, et al., Growth of 4H-SiC epilayers with low surface roughness and morphological defects density on 4 off-axis substrates [J], *Appl. Surf. Sci.* 270 (2013) 301–306.
- [22] G. Yan, Y. He, Z. Shen, et al., Effect of C/Si ratio on growth of 4H-SiC epitaxial layers on on-axis and 4 off-axis substrates [J], *J. Cryst. Growth* 531 (2020) 125362.
- [23] S. Leone, H. Pedersen, A. Henry, et al., Thick homoepitaxial layers grown on on-axis Si-face 6H-and 4H-SiC substrates with HCl addition [J], *J. Cryst. Growth* 312 (1) (2009) 24–32.
- [24] X. Liu, G. Yan, B. Liu, et al., Process optimization for homoepitaxial growth of thick 4H-SiC films via hydrogen chloride chemical vapor deposition [J], *J. Cryst. Growth* 504 (2018) 7–12.
- [25] H. Pedersen, S. Leone, A. Henry, et al., Very high growth rate of 4H-SiC epilayers using the chlorinated precursor methyltrichlorosilane (MTS) [J], *J. Cryst. Growth* 307 (2) (2007) 334–340.
- [26] Y. Niu, X. Tang, L. Sang, et al., The influence of temperature on the silicon droplet evolution in the homoepitaxial growth of 4H-SiC [J], *J. Cryst. Growth* 504 (2018) 37–40.
- [27] Y. Li, Z. Zhao, Z. Zhu, et al., Aluminum doping property in SiC epilayers grown at high growth rate using chloride-based CVD [J], *J. Mater. Sci.: Mater. Electron.* 26 (2015) 2338–2342.
- [28] K. Masumoto, C. Kudou, K. Tamura, et al., Growth of silicon carbide epitaxial layers on 150-mm-diameter wafers using a horizontal hot-wall chemical vapor deposition [J], *J. Cryst. Growth* 381 (2013) 139–143.
- [29] L. Zhao, Surface defects in 4H-SiC homoepitaxial layers [J], *Nanotechnol. Precis. Eng.* 3 (4) (2020) 229–234.
- [30] Y. Saitoh, H. Itoh, K. Wada, et al., 150 A SiC V-groove trench gate MOSFET with 6 × 6 mm² chip size on a 150 mm C-face in-house epitaxial wafer [J], *Jpn. J. Appl. Phys.* 55 (4S) (2016) 04ER05.
- [31] Z. Zhao, Y. Li, Y. Wang, et al., 4H-SiC trench filling by chemical vapor deposition using trichlorosilane as Si-species precursor [J], *J. Cryst. Growth* 607 (2023) 127104.
- [32] W. Ji, P. Lofgren, C. Hallin, et al., Computational modeling of SiC epitaxial growth in a hot wall reactor [J], *J. Cryst. Growth* 220 (4) (2000) 560–571.
- [33] H. Saitoh, T. Kimoto, H. Matsunami, Uniformity improvement in SiC epitaxial growth by horizontal hot-wall CVD [C], *Mater. Sci. Forum* (2003) 185–188.
- [34] Z. Tang, L. Gu, H. Ma, et al., Influence of temperature and flow ratio on the morphology and uniformity of 4H-SiC epitaxial layers growth on 150 mm 4° off-axis substrates [J], *Crystals* 13 (1) (2023) 62.
- [35] R. Abdulkadirov, P. Lyakhov, Estimates of mild solutions of Navier–Stokes equations in weak Herz-type Besov–Morrey spaces [J], *Mathematics* 10 (5) (2022) 680.
- [36] H. Fujibayashi, M. Ito, H. Ito, et al., Development of a 150 mm 4H-SiC epitaxial reactor with high-speed wafer rotation [J], *Appl. Phys. Express* 7 (1) (2013) 015502.
- [37] M. Ito, H. Fujibayashi, H. Ito, et al., Simulation study of high-speed wafer rotation effects in a vertical reactor for 4H-SiC epitaxial growth on 150 mm substrates [C], *Mater. Sci. Forum* (2014) 171–174.
- [38] Jones A.C., Hitchman M.L. *Chemical vapour deposition: precursors, processes and applications*[M]. Royal society of chemistry, 2009.
- [39] H. Tsuchida, I. Kamata, T. Miyazawa, et al., Recent advances in 4H-SiC epitaxy for high-voltage power devices [J], *Mater. Sci. Semicond. Process.* 78 (2018) 2–12.
- [40] T.G. Mihopoulos, S.G. Hummel, K.F. Jensen, Simulation of flow and growth phenomena in a close-spaced reactor [J], *J. Cryst. Growth* 195 (1-4) (1998) 725–732.
- [41] M. Kushibe, Y. Ishida, H. Okumura, et al., Competitive growth between deposition and etching in 4H-SiC CVD epitaxy using quasi-hot wall reactor [C], *Mater. Sci. Forum* (2000) 169–172.
- [42] B. Liu, G.-S. Sun, X.-F. Liu, et al., Fast homoepitaxial growth of 4H-SiC films on 4° off-axis substrates in a SiH₄-C₂H₄-H₂ system [J], *Chin. Phys. Lett.* 30 (12) (2013) 128101.
- [43] J. Hu, R. Jia, B. Xin, et al., Effect of low pressure on surface roughness and morphological defects of 4H-SiC epitaxial layers [J], *Materials* 9 (9) (2016) 743.
- [44] L. Zhao, H. Wu, A correlation study of substrate and epitaxial wafer with 4H-N type silicon carbide [J], *J. Cryst. Growth* 507 (2019) 109–112.
- [45] M. Yazdanfar, P. Stenberg, I. Booker, et al., Process stability and morphology optimization of very thick 4H-SiC epitaxial layers grown by chloride-based CVD [J], *J. Cryst. Growth* 380 (2013) 55–60.
- [46] S. Zhao, J. Wang, G. Yan, et al., Surface uniformity of wafer-scale 4H-SiC epitaxial layers grown under various epitaxial conditions [J], *Coatings* 12 (5) (2022) 597.
- [47] Y. Li, Z. Zhao, L. Yu, et al., Reduction of morphological defects in 4H-SiC epitaxial layers [J], *J. Cryst. Growth* 506 (2019) 108–113.
- [48] D. Baierhofer, B. Thomas, F. Staiger, et al., Defect reduction in SiC epilayers by different substrate cleaning methods [J], *Mater. Sci. Semicond. Process.* 140 (2022) 106414.
- [49] M. Yazdanfar, S. Leone, H. Pedersen, et al., Carrot defect control in chloride-based CVD through optimized ramp up conditions [C], *Mater. Sci. Forum* (2012) 109–112.
- [50] J. Hassan, A. Henry, P. McNally, et al., Characterization of the carrot defect in 4H-SiC epitaxial layers [J], *J. Cryst. Growth* 312 (11) (2010) 1828–1837.
- [51] Y. Mabuchi, T. Masuda, D. Muto, et al., Investigation of carrot reduction effect on 4H-silicon carbide epitaxial wafers with optimized buffer layer [C], *Mater. Sci. Forum* (2017) 75–78.
- [52] H. Pedersen, S.T. Barry, J. Sundqvist, Green CVD—toward a sustainable philosophy for thin film deposition by chemical vapor deposition [J], *J. Vac. Sci. Technol. A* 39 (5) (2021).
- [53] J. Guo, Y. Yang, B. Raghathamachar, et al., Understanding the microstructures of triangular defects in 4H-SiC homoepitaxial [J], *J. Cryst. Growth* 480 (2017) 119–125.
- [54] Y. Daigo, T. Watanabe, A. Ishiguro, et al., Reduction of harmful effect due to by-product in CVD reactor for 4H-SiC epitaxy [C], 2020 Int. Symp. Semicond. Manuf. (ISSM) (2020) 1–4.
- [55] S.-I. Nakashima, H. Harima, Raman investigation of SiC polytypes [J], *Phys. Status Solidi (a)* 162 (1) (1997) 39–64.
- [56] Y. Daigo, A. Ishiguro, S. Ishii, et al., Reduction of surface and PL defects on n-type 4H-SiC epitaxial films grown using a high speed wafer rotation vertical CVD tool [C], *Mater. Sci. Forum* (2018) 108–111.
- [57] Y. Daigo, T. Watanabe, A. Ishiguro, et al., Influence and suppression of harmful effects due to by-product in CVD reactor for 4H-SiC epitaxy [J], *IEEE Trans. Semicond. Manuf.* 34 (3) (2021) 340–345.